Princeton Plasma Physics Laboratory

PPPL-5184

A correlation between morphology of the carbonaceous deposit and the current distribution in the carbon arc discharge for nanosynthesis

Yao-Wen Yeh[a, b*], Yevgeny Raitses[a], and Nan Yao[b]

[a] Princeton Plasma Physics Laboratory, Princeton University, P.O. Box 451, Princeton, NJ 08543, USA

[b] Princeton Institute for Science and Technology of Materials, Princeton University, Princeton, NJ 08544, USA

August 2015

Prepared for the U.S. Department of Energy under Contract DE-AC02-09CH11466.

Princeton Plasma Physics Laboratory
Report Disclaimers

Full Legal Disclaimer

Trademark Disclaimer

PPPL Report Availability

Princeton Plasma Physics Laboratory:

http://www.pppl.gov/techreports.cfm

Office of Scientific and Technical Information (OSTI):

http://www.osti.gov/scitech/

Related Links:

U.S. Department of Energy

U.S. Department of Energy Office of Science

U.S. Department of Energy Office of Fusion Energy Sciences

A correlation between morphology of the carbonaceous deposit and the current distribution in the carbon arc discharge for nanosynthesis

Yao-Wen Yeh[a, b*], Yevgeny Raitses[a], and Nan Yao[b]

[a] Princeton Plasma Physics Laboratory, Princeton University, P.O. Box 451, Princeton, NJ 08543, USA
[b] Princeton Institute for Science and Technology of Materials, Princeton University, Princeton, NJ 08544, USA

Abstract

Synthesis of carbon nanotubes by atmospheric pressure arc discharge involves ablation of the graphite anode and deposition of carbonaceous products on the cathode surface. This cathode deposit exhibits distinct spatial structural variations. In particular, three different morphologies with an axial symmetry where a rim of pyrolytic carbon separates the innermost core with multiwalled carbon nanotubes from the outermost ring with powdery amorphous carbon soot. It is shown experimentally that there is a strong correlation between the arc current distribution at the cathode, the temperature of the deposit, and the nanotube forming area.

1. Introduction

Carbon nanotubes are of great interest in both technology and fundamental science because of their attractive material properties and their one-dimensional structure.[1,2] Without using metal catalysts, multiwalled carbon nanotubes (MWCNTs) are found in the carbonaceous materials deposited on the cathode by carbon arc discharge.[3,4] The structure of the tube was first discussed in detail by Ijjima[3] and has attracted great attention ever since. While MWCNTs are abundant, it is also known that they are not the only carbon products synthesized by arc discharge.[4,5] In particular, the cathode deposit consists of a soft fibrous core that contains MWCNTs and a hard shell that is made of pyrolytic graphitic sheets.[4–6] While the role of cathode deposit in the carbon arc has been reported to serve as an effective cathode during the arc discharge,[7] there are a number of questions that remain unanswered. For example, it is still unclear why the deposit forms with such distinct morphologies. What are the local plasma conditions during the discharge that lead to the deposit formation?

In recent studies,[7–9] we reported that for the same current, the dependence of the graphite anode ablation rate on the anode diameter is highly non-linear and does not follow the arc current density

* Corresponding author.
E-mail address: yyeh@princeton.edu (Y Yeh)
Telephone number: 609-258-6878 (Y. Yeh)

at the anode. In particular, we showed the existence of a critical anode diameter (or the current density at the anode), for which the anode ablation rates of smaller diameter anodes increase sharply reaching more than ten times of the ablation rates of larger anodes.[9] As a result, the cathode deposit for a smaller anode is thicker than the cathode deposit for a larger anode. The switching from low to high ablation mode was attributed to the transition of the anode sheath, located between the plasma and the anode, from negative (electron repelling) to positive (electron attracting).[8] However, independent of the difference in ablation and deposition rates, the cathode deposits produced under these two modes have the same general features, namely a fibrous core at the center of the deposit and the hard shell with soot like deposit outside the core.[4,5]

Previously, we reported that the arc current was conducted through the small area across from the anode, in spite of the cathode size being larger than the anode.[7] Building upon the observed current distribution and distinct axial structural variation of the cathode, we aim to study the interconnection between the spatial characteristic of the arc and the deposit properties in greater detail. The paper is organized as follows: in Section 2, we describe the experimental method. Experimental results and analysis are discussed in Section 3, followed by conclusions. The main result of the present study is that there is a strong correlation between the arc current distribution at the cathode, the temperature of the deposit, and the nanotube forming area.

2. Experimental

The experimental setup with the segmented cathode is shown in **Fig. 1**. The experimental apparatus employed in the present study has already been described elsewhere.[7–9] The anode (A) and cathode (C) were set up in a vertical configuration in order to avoid asymmetrical effects on the arc and deposition brought by convective flow. The segmented cathode was composed of a graphite central electrode (diameter d = 3.2 mm) and a copper rim electrode (d = 50.8 mm). The rim electrode is insulated from the central electrode by a thin layer of boron nitride with a thickness of 0.5 mm in order to minimize the disturbance to the arc. It should be noted that the presence of the boron nitride layer did not affect the deposit morphologies compared to the deposit observed on a normal cathode. Discharges with a regular copper cathode (d = 50.8 mm) and small graphite cathode (d = 3.2 mm) were also run.

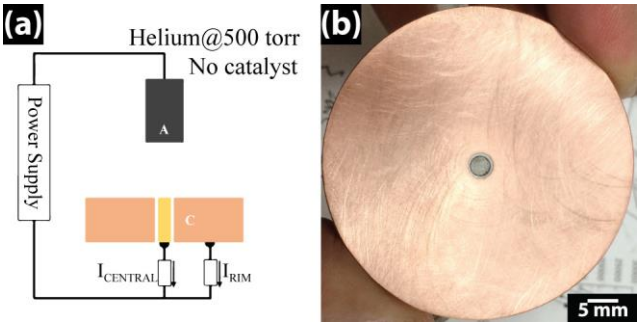

Fig. 1 (a) Simplified schematic of the arc setup with graphite anode (A) and the segmented cathode (C). (b) Photograph of the segmented cathode.

The carbon arc discharge experiments were conducted in a chamber filled with helium gas at 500 Torr. A discharge voltage of about 20 V was maintained on the electrodes during the arc. The arc was initiated by bringing the anode into contact with the cathode, after which the current was maintained at 65 A and the control system increased the electrode gap until the specified discharge voltage was reached. The gap was about 2 mm wide. It took about 10 s for the arc current to stabilize and for the anode to reach the specified gap. During the arc, the graphite anode ablates, producing ablated carbonaceous products, including atoms, molecules and various particles, which are transported in the arc to the cathode to form a carbonaceous deposit as shown in **Fig. 2.**

While the high anode ablation employed in typical carbon nanotube synthesis leads to large-scale tube synthesis,[4,5,10] it also presents a challenge to study local cathode conduction (such as cathode current distribution) since the deposit grows quickly. Thus, the anode diameter was chosen such that the arc operated with a low ablation and deposition rates which facilitated the study of the current distribution at the cathode. With an anode diameter of 9 mm as used in the present study, the arc was operated in low ablation mode and had a rate of 0.56 ± 0.03 mg/s and typical thickness of the deposit was about 1 mm.

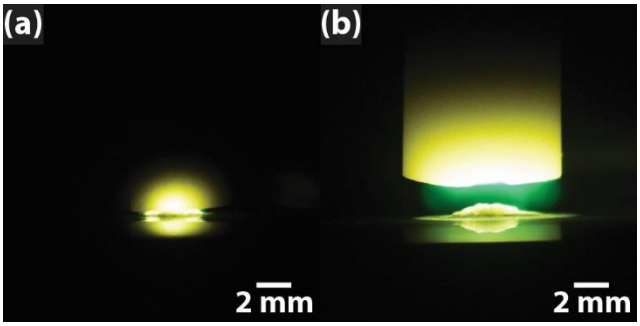

Fig. 2. Optical images of (a) the onset of the arc and (b) arc steady state. The top and bottom electrodes are anode and cathode, respectively. The small hump of the material on the cathode is the deposit.

In addition to the current distribution measurements, the deposit temperature distribution was monitored during the arc discharge. The temperature distribution was measured by a calibrated FLIR tau 2 640 infrared camera together with a 3.2% transmittance neutral density filter. Similar to the calibration procedure reported earlier,[7,9] we used C-type thermocouples inserted into the anode and the cathode to calibrate this IR camera. The temperature measured by the IR camera had an uncertainty of 100°C. In addition, these thermocouples were used in order to determine the heat flux to the electrodes.

The cathode deposits produced in arc experiments were carefully studied via electron microscopy. In order to have more complete picture of the materials synthesized, the cathode deposit from each run was kept on the cathode without disturbance and first surveyed by an FEI Quanta 200 field emission SEM operated at 5 kV. Each part of the deposit was then separately collected, sonicated in an acetone bath for about 3 minutes, and dispersed onto a TEM grid. The TEM samples were studied by a Philip CM200 field emission TEM at 200 kV. It was noted that the deposits obtained on the segmented and the regular cathodes show the general fibrous core and hard shell features without noticeable differences, and that the presence of the boron nitride layer did not affect the deposit morphologies observed on a normal cathode. Finally, structural analysis of the deposit was carried out by a Rigaku MiniFlex XRD with Cu Kα as the x-ray source.

3. Results and discussion

3.1 Cathode deposit

During the arc operation, the carbon anode is ablated, and the ablated materials are subsequently deposited onto the cathode surface. Without metal catalysts, the cathode deposit is the main product produced by the arc, and there is no web-like material observed around the electrodes.[4,5,11] This deposit contains carbon nanostructures. As shown in **Fig. 3a**, three general and distinct features of the deposit are identified. Starting from the innermost to the outermost part, the deposit consists of (1) a fibrous core that contains loosely entangled and randomly oriented MWCNTs and polyhedral carbon nanoparticles (CNPs), (2) a particulate rim that contains curvy pyrolytic carbon sheets, and (3) amorphous carbon soot. The nanotubes were found only in the core area of the deposit. While the morphologies of the thin pyrolytic carbon rim look similar to the outermost amorphous soot, subsequent TEM and XRD characterizations revealed their structural difference. The detailed electron images of the fibrous core, pyrolytic carbon rim, and

amorphous carbon are shown in **Fig. 3b**, **3c**, and **3d**, respectively. The fibrous core and the particulate rim accounted for about 60% of the ablated anode mass.

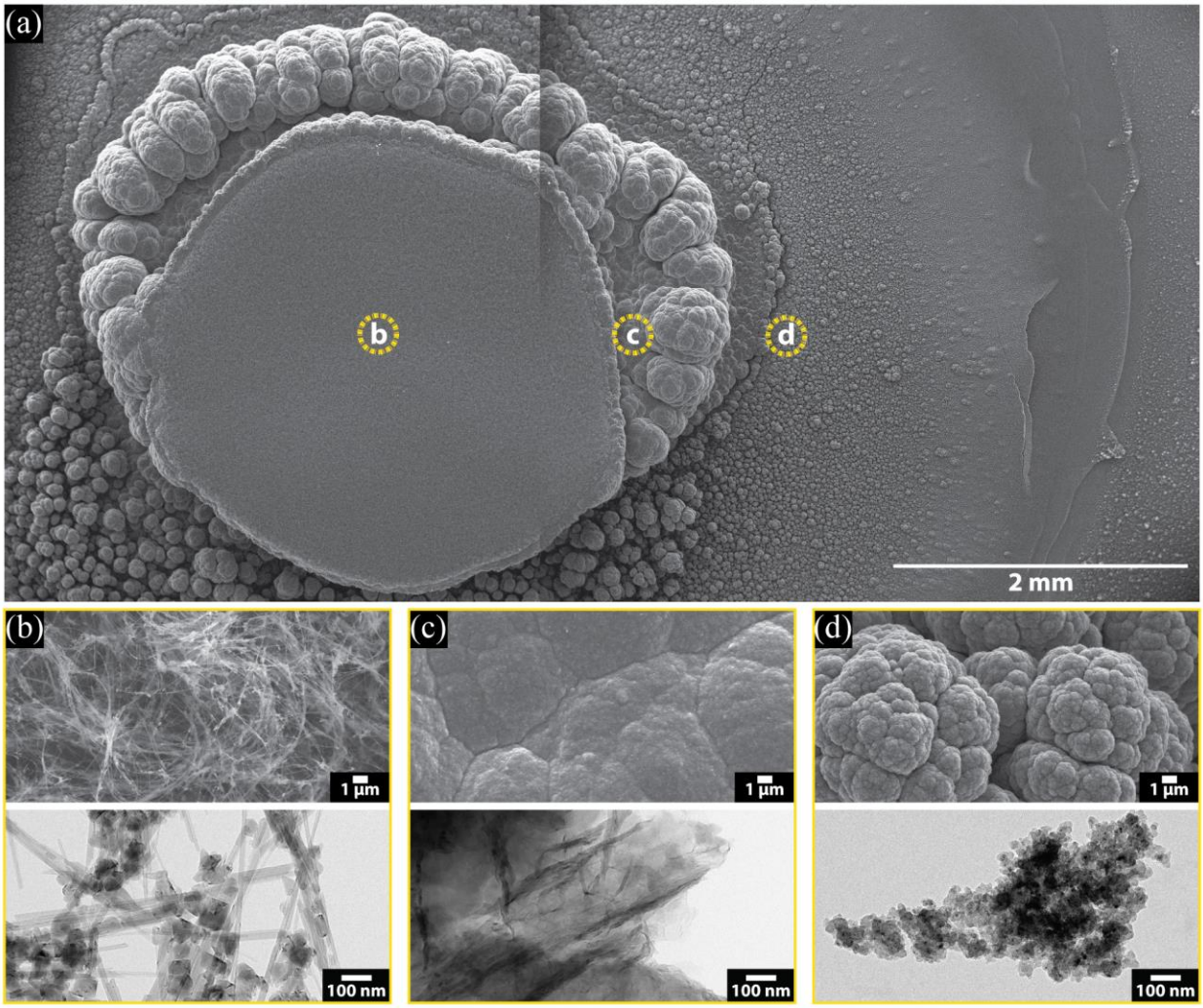

Fig. 3. Electron micrographs of a cathode deposit. (a) Three regions can be distinguished based on their different morphologies – (b) the fibrous core that contains MWCNTs and CNPs only, (c) particulate rim that contains pyrolytic carbon sheets, and (c) amorphous carbon soot.

3.2 Structural analysis by XRD

The structural characterization of the cathode deposit and the starting graphite materials were carried out by Rigaku MiniFlex XRD. As shown in **Fig. 4**, while the deposit core and rim materials are different in morphologies, they show the same turbostratic graphitic structure with the absence in c-axis ordering indicated by the missing (101) and (112) peaks that are observed from the starting anode material.[1,10] Both the core and rim materials show (002) interlayer spacing to ~3.4 Å. The full-width-half-maxima of the (002) peak are 0.6 and 0.9 degrees for the deposit core and rim materials, respectively. The narrower (002) FWHM observed in the core material indicates

that the core has higher crystallinity than the rim material, which in turn suggests that the forming temperature of the core was higher than the rim. As will be discussed later, the observation agrees with the deposit temperature measurement during the discharge. The amorphous nature of the soot material was confirmed by the XRD pattern. The two peaks at 44.24° and 81.96° observed from the deposit soot material are from copper (110) and (211), respectively, which indicated that trace amount of copper was vaporized during the discharge. Using the graphite as the reference, the diffraction peaks of each part of the deposit are summarized in **Table 1**.

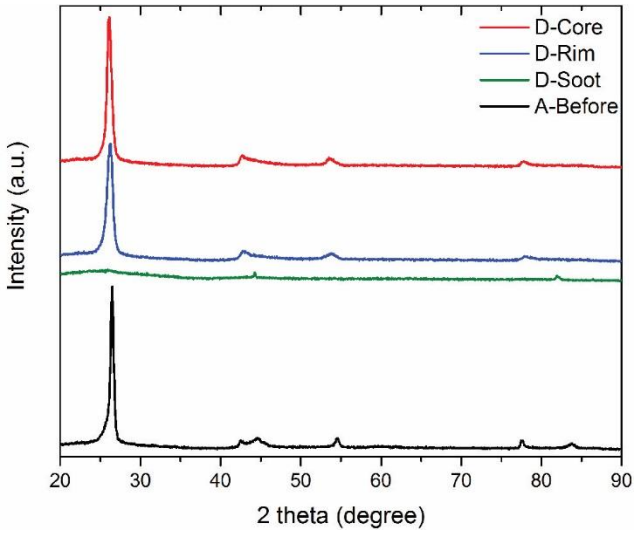

Fig. 4. XRD patterns stating from the top to bottom are the fibrous core of the deposit (D-Core), the pyrolytic carbon rim (D-Rim), the starting graphite anode (A-Before), and the carbon soot of the deposit (D-soot).

Table 1. Typical XRD results of the starting graphite and the cathode deposit. The deposit is broken down into the fibrous core (D-Core), hard rim (D-Rim), and the soot (D-Soot)

Sample	d_{002} (Å)	d_{100} (Å)	d_{101} (Å)	d_{004} (Å)	d_{110} (Å)	d_{112} (Å)
Graphite	3.363	2.126	2.034	1.683	1.230	1.154
D-Core	3.409	2.115	n/a	1.712	1.230	n/a
D-Rim	3.390	2.113	n/a	1.708	1.226	n/a
D-Soot	n/a	n/a	n/a	n/a	n/a	n/a

3.3 Cathode current distribution

Building upon previous work,[7] the segmented cathode was used to monitor the current distribution during the arc. Unlike the previous work,[7] the diameter of the central electrode used in the present work was nearly twice smaller, 3.2 mm. This is in order to study the cathode current conduction with a higher resolution than in **Ref. 5**. For each run, the arc was operated for 30 s.

The duration was chosen to be long enough for the arc to reach steady state, and to avoid a large deposit, which could short the electrodes. The arc current took around 10 s to stabilize, as indicated in **Fig. 5a**. With high reproducibility, it is found that the majority of the total current (70% - 95%) was conducted through the central segmented-electrode. The spread of the measured current through this electrode was caused by variations of the placement of the arc attachment to the cathode for different arc runs. Consequently, the physical center of the arc discharge and its attachment to the cathode could deviate from the geometrical center of the segmented cathode. This deviation caused a shift of the arc attachment with respect to the central cathode.

Importantly, it was found that the cathode deposit on the central electrode only contained MWCNTs and CNPs. This was actually the only deposit region containing nanotubes. In fact, **Fig. 5b** shows that while the deposit collected after the discharge has a diameter of 14 mm, only the smaller central cathode area contained MWCNTs. Thus, there is a strong correlation between the current conducting area and the area where MWCNTs form.

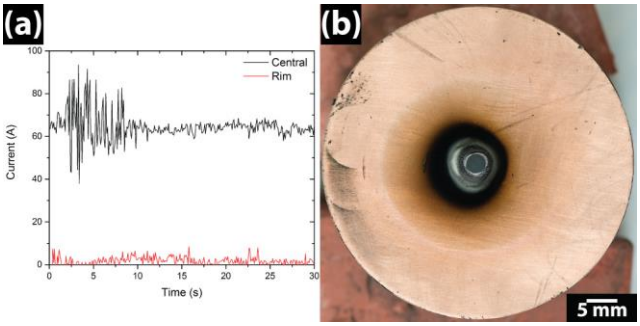

Fig. 5. (a) Current distribution plot from one experiment. The black and red lines are the cathode currents through the core and rim electrode, respectively. (b) The cathode after arc discharge experiment.

3.4 Cathode deposit temperature and structure

During the arc discharge, the temperature of the cathode deposit can be as high as 3500 K, as shown in **Fig. 6a** and **6b**. The deposit region with such high surface temperature corresponds to the placement of the central segmented electrode. The average surface temperature in this region is 3100 K.

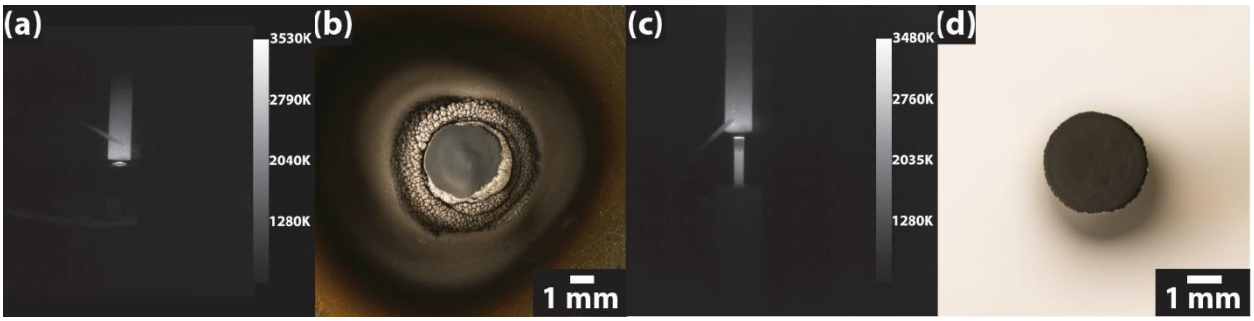

Fig. 6. Thermographs and deposit materials for (a, b) the segmented cathode and (c, d) the d = 3.2 mm graphite cathode.

In addition to the segmented cathode, a small graphite cathode (d = 3.2 mm) was used in order to check if the three structural variations of the cathode deposit that were observed on the large cathode (d = 50.8 mm) were universal. The average surface temperature of the deposit on the small cathode was similar to the deposit on the large cathode. However, the deposit found on the small cathode surface had only MWCNTs and CNPs, without the pyrolytic carbon rim and soot as in the case of the large cathode. Extracting the minimum and maximum temperatures observed from the tube containing core, the measurements suggest that the nanotubes could form and withstand the temperatures between 2700 K and 3500 K. The lower bound of the observed temperature range is similar to the value reported by Liang *et al* who studied the nanotube-forming temperature at the anode surface during the arc.[12]

Fig. 7 shows radial distribution of the deposit surface temperature deduced from measurements with the infrared camera (**Fig. 6a**). The temperature has a maximum at the center of the deposit. A relatively strong temperature decrease is observed at the distance 1.5 mm from the center, which corresponds to the boundary between the MWCNT core and the pyrolytic rim (**Fig. 6b**). The temperature drop may be attributed to the radial profile of the heat flux from the plasma.

As shown in **Fig. 2b**, the deposit accumulates more material at the center to form a hump on the cathode. Huczko *et al.*[13] reported that for fullerene synthesis condition (helium at 100 Torr), both the temperature and the density of carbon radical (C_2) in the arc column have their maximum values at the center of the plasma column. While the helium pressure used in the present study is 500 Torr, the observed profile of the cathode deposit may be also attributed to larger temperature and density of carbon radicals at the center of the arc. The formation of MWCNTs is affected not only by the temperature of the deposit, but also by the carbon flux distribution from the plasma to the cathode. Furthermore, these variations of the deposit morphology are likely associated with the

radial distribution of the heat conduction from the plasma to the cathode.[7] According to **Refs. 7** and **12**, the heat conduction from the plasma to the cathode is the main heat source contributing to the energy balance at the cathode.

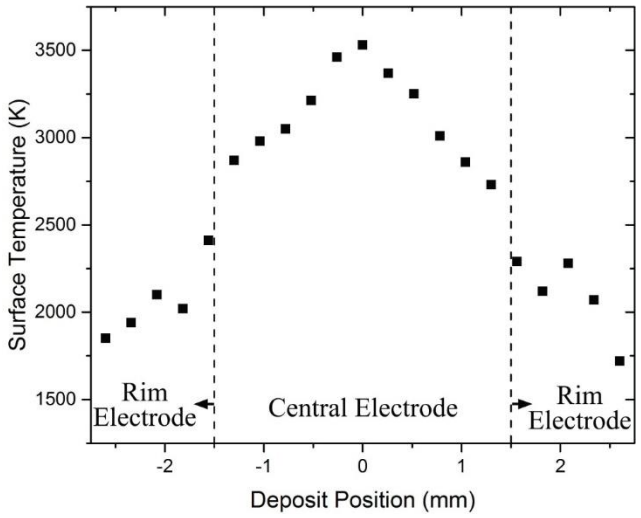

Fig. 7. Surface temperature profile of the cathode deposit during the arc. The profile shows radial symmetry where the highest temperature locates at the deposit center. The dash lines indicates the boundary between the nanotube forming core (the central electrode) and the pyrolytic carbon and soot depositing area (the rim electrode).

4 Conclusion

The arc discharge for synthesis of carbon nanomaterials involves the ablation of the graphite anode and the deposition of the ablated products on the cathode surface. It is shown that the carbon deposit on the cathode surface consists of three different morphologies: (1) a center MWCNT core, enclosed by (2) a particulate pyrolytic carbon rim, which is surrounded by (3) amorphous carbon soot. Measurements of the arc current at the cathode and the deposit temperature revealed a strong correlation between the radial distribution of the arc current, the deposit surface temperature, and variations of structural morphology of the deposit. In particular, it was found that more than 70% of the total arc current is conducted through the deposit core area where the MWCNTs are formed. It is suggested that this correlation is associated with the radial distribution of the heat flux from the plasma, which reaches its maximum at the center of the deposit, where the temperature is maximum. Finally, these results also suggest that the MWCNTs formed on the deposit can survive the temperatures between 2700 K and 3500 K.

Acknowledgements

The authors wish to thank Mr. Jonathan Ng, Dr. Sophia Gershman, and Prof. Bruce Koel for fruitful discussions. We also thank Mr. Alex Merzheskiy for his technical support of this work. This work was supported by U.S. Department of Energy, Office of Science, Basic Sciences, Materials Sciences and Engineering Division and the National Science Foundation-MRSEC program through the Princeton Center for Complex Materials (DMR-0819860).

References

[1] G. Dresselhaus, M.S., Dresselhaus, *Carbon Nanotubes Synthesis, Structure, Properties, and Applications* (Springer-Verlag, Berlin, 2001).

[2] C. Fisher, A.E. Rider, Z. Jun Han, S. Kumar, I. Levchenko, and K. Ostrikov, J. Nanomater. **2012**, (2012).

[3] S. Iijima, Nature **354**, 56 (1991).

[4] P.M. Ajayan, P. Redlich, and M. Rühle, J. Mater. Res. **12**, 244 (1997).

[5] D. Tang, L. Sun, J. Zhou, W. Zhou, and S. Xie, Carbon **43**, 2812 (2005).

[6] G. Gamaly and T.W. Ebbesen, Phys. Rev. **52**, 2083 (1995).

[7] J. Ng and Y. Raitses, Carbon **77**, 80 (2014).

[8] A.J. Fetterman, Y. Raitses, and M. Keidar, Carbon **46**, 1322 (2008).

[9] J. Ng and Y. Raitses, J. Appl. Phys. **117**, 063303 (2015).

[10] Y. Saito, T. Yoshikawa, M. Inagaki, M. Tomita, and T. Hayashi, Chem. Phys. Lett. **204**, 277 (1993).

[11] P.J.F. Harris, Carbon **45**, 229 (2007).

[12] F. Liang, M. Tanaka, S. Choi, and T. Watanabe, J. Chem. Eng. Japan **47**, 296 (2014).

[13] A. Huczko, A. Huczko, H. Lange, H. Lange, P. Byszewski, P. Byszewski, M. Poplawska, M. Poplawska, A. Starski, and A. Starski, J. Phys. Chem. A **101**, 1267 (1997).

PPPL PRINCETON PLASMA PHYSICS LABORATORY

Princeton Plasma Physics Laboratory
Office of Reports and Publications

Managed by
Princeton University

under contract with the
U.S. Department of Energy
(DE-AC02-09CH11466)

P.O. Box 451, Princeton, NJ 08543
Phone: 609-243-2245
Fax: 609-243-2751

E-mail: publications@pppl.gov

Website: http://www.pppl.gov